An investigation of potential wear occurring on refractory lining and coating formation- a remedy of wear in a basic oxygen steelmaking furnace using CFD modelling

R. Chowdhury[1,7], S. Mitra[2,7], G. Evans[3,7], T. Honeyands[4,7], B. J. Monaghan[5], D. Scimone[6,7]

1. Research Assistant, University of Newcastle, Callaghan, NSW 2308, Australia.
   Email: raju.chowdhury@newcastle.edu.au
2. Research Academic, University of Newcastle, Callaghan, NSW 2308, Australia.
   Email: subhasish.mitra@newcastle.edu.au
3. Conjoint Professor, University of Newcastle, Callaghan, NSW 2308, Australia.
   Email: geoffrey.evans@newcastle.edu.au
4. Associate Professor, University of Newcastle, Callaghan, NSW 2308, Australia.
   Email: tom.a.honeyands@newcastle.edu.au
5. Professor, University of Wollongong, NSW 2522, Australia.
   Email: monaghan@uow.edu.au
6. Senior Refractory Technologist, BlueScope Steel, Port Kembla, NSW 2505, Australia.
   Email: David.Scimone@bluescopesteel.com
7. ARC Research Hub for Australian Steel Manufacturing, University of Wollongong, NSW 2500, Australia.

Keywords: Basic Oxygen Steelmaking, refractory wear, slag splashing, coating formation, CFD modelling

ABSTRACT

Due to the harsh operating conditions, wearing of the inner refractory lining in a Basic Oxygen Steelmaking (BOS) furnace reduces the useful life of the refractories and incurs a significant cost component for relining. In this study, firstly, a combined compressible and incompressible computational fluid dynamics (CFD) model was developed to identify the potential wear prone zones in an industrial scale BOS system during the supersonic oxygen blowing phase by quantifying the wall shear stress distributions. Next, the retained slag splashing process was simulated by introducing an inert gas to residual slag mass to achieve a protective coating on the refractory walls. Effect of both design and operational parameters such as lance head configuration, lance position and the initial slag volume on the slag wall coating performance were quantified and most favourable conditions were determined.

1. INTRODUCTION

Wearing of the inner refractory lining of the Basic Oxygen Steelmaking (BOS) furnace is a known problem in the steelmaking industry. It reduces the useful life of BOS refractories. Replacing or repairing the refractory lining is quite a capital-intensive issue. Timely identification of the potential wear prone zones allows deployment of some targeted wear mitigation strategies to prolong the overall life of the furnace's working refractory lining.

BOS steelmaking is a complex process where oxygen gas is injected at a supersonic speed through a lance comprising multiple converging-diverging nozzles into a molten iron bath to reduce the carbon content and remove the impurities from the liquid metal phase to slag phase by oxidisation. The supersonic gas jet exhibits complex interactions with the liquid metal and slag phase involving deformation of slag/metal interface, cavity formation, bath oscillation, droplet generation, and chemical reactions (Li et al., 2016a). The rate of the oxidation reactions greatly depends on the mixing of oxygen gas with the hot metal and is governed by momentum transfer from the gas jet which produces oscillatory motions in the liquid. The slag foaming (gas-slag-metal emulsions) that forms due to the chemical reactions influences the mixing performance by accelerating the process kinetics (Sattar et al., 2014). The gas jet velocity that controls the mixing performance mainly depends on the nozzle design (Fruehan, 1998). Wear occurs in the inner lining of the converter over a prolonged period of operation due to the combined effect of chemical, mechanical and thermal attacks. Among these causes, mechanical wear occurs due to the bath oscillation motion during the steel refining process (Li et al., 2016b). Wear does not occur uniformly within the furnace; rather, it occurs locally and depends on the wall shear stress generated during the steelmaking operation.

Previously, some numerical studies have been conducted by (Odenthal et al., 2006, Li et al., 2016b, Sun et al., 2022) to investigate the hydrodynamic behaviour of the main blowing process in a full-scale BOS system. These studies mainly examined the cavity profile, mixing time and effect of lance height variation, lance designs, and bottom tuyere arrangements. A few of these studies (Li et al., 2016b, Sun et al., 2022) specifically quantified the wear prone zones due to the bath oscillation. (Li et al., 2016b) identified the wearing zone to exist between the slag-free surface and slag-metal interface while (Lee et al., 2001) reported that wear occurs at the knuckle region of the BOS furnace based on experiment.

Effective coating formation on the wearing zones ensures higher productivity by prolonging the life span of a BOS furnace. Slag splashing is a known cost effective remedy for such purpose (Fruehan, 1998, Mills et al., 2005) compared to other coating formation methods such as gunning and slag coating. In this process, an inert gas such as nitrogen is blown through the lance into the retained slag pool periodically. The gas jet-slag interaction generates numerous slag droplets which deposit on the refractory wall, solidify, and form a protective coating layer on the furnace wall. This process can be enhanced by adding bottom bubbling through the tuyeres mounted on the furnace floor (Mills et al., 2005). Achieving a good coating layer is case specific and depends on the slag composition, gas flow rate, quantity of residual slag, lance head design, lance position, converter shape and dimensions.

In slag splashing process, the main purpose is to coat a targeted region of BOS furnace utilising the optimal volume of slag in the shortest possible time. Determining such conditions through plant trials is quite expensive (Luomala et al., 2002). Some past numerical studies (Barron et al., 2015, Leão et

al., 2016, Sinelnikov et al., 2021) investigated the potential of slag splashing method by assessing the influence of above stated operating conditions. It is however noted that these investigations focused on high gas flow rate ($Ma = 1$ or $Ma > 1$, where Ma is the Mach number- defined as the ratio of flow speed to the sound speed) while studies on the low flow rate ($Ma < 1$) scenarios with industrial conditions were quite limited. To address this knowledge gap, the present study aims to develop a comprehensive CFD model to investigate the hydrodynamic behaviour in an industrial scale BOS furnace utilising the actual operating conditions and determine the potential wear prone zones. Also, the study aims to quantify the effect of different operating conditions on the coating formation.

2. NUMERICAL MODELLING

A Computational Fluid Dynamics (CFD) model of an industrial scale BOS system was developed on the commercial CFD solver ANSYS-Fluent platform to simulate two main scenarios – a normal oxygen injection operation to determine the wear prone zones inside the furnace and a slag splashing operation with inert gas injection from both furnace top and bottom. The entire CFD modelling framework presented in this paper was divided into two separate parts comprising a compressible flow and incompressible flow component, respectively.

2.1 Flow modelling of lance head

First, a single phase CFD model was developed to quantify the flow behaviour in a 3D converging-diverging (CD) nozzle in the lance head of two different designs comprising 5 and 6 nozzles, as well as bottom tuyeres. The model included continuity, momentum, and energy equations which were simultaneously solved using a compressible flow solver on a fixed Eulerian structured mesh. To account for the turbulence effect, a two-equation SST (shear stress transport) k–ω model was utilised. To simulate the high heat transfer rate between the impinging gas jet and the liquid metal, the value of turbulent Prandtl number was set to $Pr_t = 0.5$ in the energy equation (Alam et al., 2010).

Taking advantage of the symmetric geometry (Fig.1a), only half domain of the lance head (Fig. 1b) and a quarter domain of the tuyere (Fig. 1c) was simulated to reduce the computational cost. A *pressure inlet* boundary condition was applied at the nozzle inlet whereas a *pressure outlet* boundary condition was applied at the outlet. A *no-slip* condition was adopted on the walls. Gas density was computed from the ideal gas law. First order upwind scheme was used to discretise the pressure, momentum, and energy equations and the solution convergence criterion for all residuals was set at 10^{-6}.

Two low-pressure gas flow rate cases (11,600 Nm^3/hr and 250 Nm^3/hr nitrogen flow through lance and tuyere, respectively) were simulated by applying *mass flow inlet* boundary condition at the inlet of lance and tuyere to determine the exit velocity and temperature. The model predicted velocity and temperature obtained at the lance and tuyere exit were used as boundary conditions for simulation of the overall hydrodynamic behaviour in a BOS system.

2.2 Flow modelling of BOS system

A 2D Eulerian-Eulerian multiphase CFD model was developed to simulate the flow dynamics of BOS system. Due to high computational cost involved in 3D modelling of a full-scale BOS system, a 2D model was instead considered. The computational domain for the main blowing process is shown in Fig. 1d. The model comprised continuity, momentum with standard k–ε turbulence closure with standard wall function, and energy equation to account for the interactions between a gas jet and pool of liquid metal and slag phase. Any chemical reactions due to phase interactions were not considered.

For the slag splashing scenario, only the lower part however was considered (Fig. 1f) keeping the governing equations same. *Velocity inlet* boundary condition was applied at the inlet and *pressure outlet* boundary condition was employed at the outlet. A no-slip condition was applied to the walls and the temperature was set to 1923 K. Solidification sub-model was not considered. Instead, it was assumed that where the slag will be in contact with the furnace wall, it will solidify.

The thermo-physical properties of BOS slag and metal used in the CFD model are given in Table 1. The properties of slag were computed using (Mills et al., 2011) for the slag compositions (Drain, 2018) provided in Table 2. Before performing CFD simulations, a grid independency test was

performed for each case considering three different grid levels to ensure the accuracy of the simulation results.

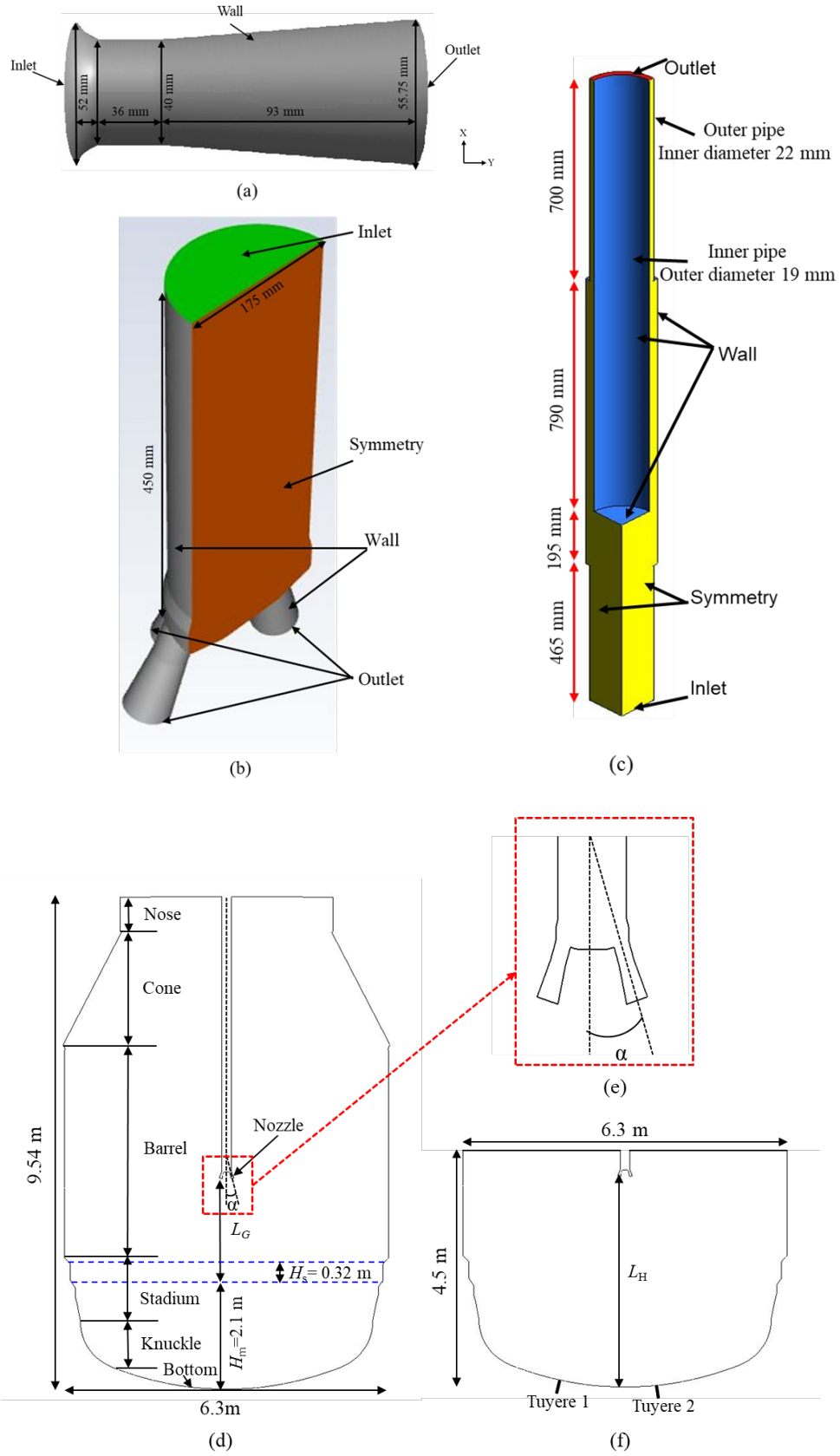

Fig 1: Computational domains (a) a 3D single CD nozzle used in *Lance*1, (b) a 3D 6 hole lance head, (c) bottom tuyere, (d) a 2D full-scale BOS furnace comprising a lance head to be used in main blowing simulation cases, (e) enlarged view of lance head, and (f) a 2D full-scale BOS furnace comprising a lance head and bottom tuyere to be used in slag splashing simulation cases.

Table 1 – Properties of slag and metal

Physical properties	Slag	Metal
Density ρ_l (kg·m^{-3})	3067	7020
Dynamic viscosity μ_l (Poise)	0.24	0.05
Temperature T (K)	1923	1923
Thermal conductivity k_l (W·m^{-1}·K^{-1})	0.05	40
Surface tension σ_l (N·m^{-1})	0.55	1.6
Specific heat Cp_l (J·kg^{-1}·K^{-1})	1414	670

Table 2 – Slag compositions

Constituents	CaO	MgO	P	SiO_2	Fe_tO^*	MnO	Al_2O_3	TiO_2	S	V_2O_5
Mass (%)	42.7	9.5	1.0	13.0	23.3	4.6	2.0	1.2	0.1	1.6

$^*Fe_tO$ represents the total Fe in slag phase as FeO

The governing equations were discretised using a first-order upwind scheme and spatial gradients were computed with a least-squares method. The pressure values at the cell faces were interpolated using the PRESTO (PREssure Staggering Option) scheme. Finally, pressure–velocity coupling was achieved by using a PC-SIMPLE (Phase Coupled Semi Implicit Pressure Linked Equation) algorithm. The initial time step size was set to 1×10^{-6} s and then switched to an adaptive scheme ensuring stability of the solution (global Courant number < 1.0). The convergence criterion was set to 1×10^{-6} for the absolute residual of energy parameter, while a value of 1×10^{-3} was set for mass flow, velocity, and turbulence parameters. All calculations were carried out on a high-performance computing Linux cluster deploying a maximum of 32 parallel processors. The required wall time was 144 h to simulate 1 s physical time for both, main blowing and slag splashing cases. Due to very long computation time required for these calculations, main blowing and slag splashing simulations were run for only 10 s and 4 s, respectively.

3. RESULTS AND DISCUSSIONS

3.1 Model validation

The developed CFD models were first validated with the theoretical solutions wherever applicable. For lance head, model predictions were validated by comparing with the isentropic theory as shown in Fig. 2a. It can be seen the CFD model predicted Mach number along the nozzle axis agrees well with the isentropic theory showing only ~ 0.13% deviation at the nozzle exit.

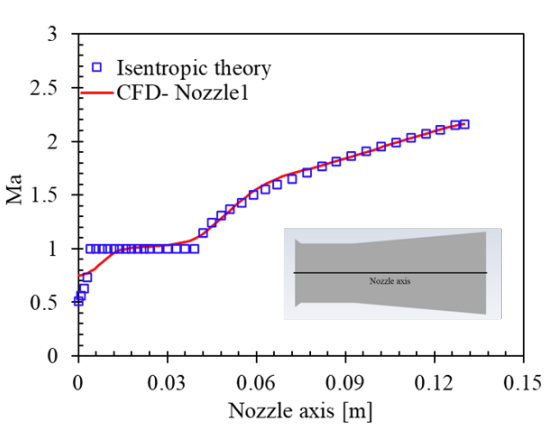

(a)

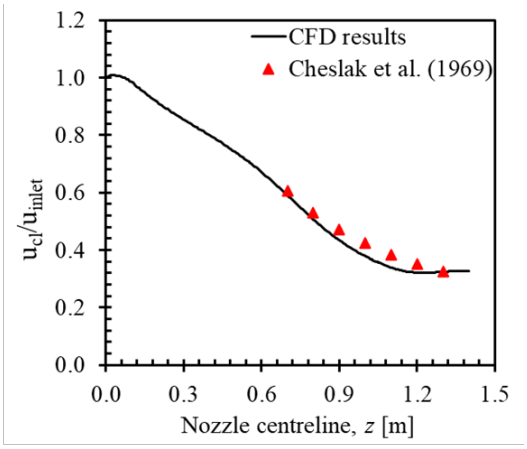

(b)

Fig 2: (a) Single phase flow model comparison with isentropic theory and (b) multi-phase flow model comparison with theoretical prediction.

For the gas jet flow simulations, the model predictions were compared with the theoretical prediction of a single gas jet decay along the nozzle centreline (Cheslak et al., 1969). The centre line gas velocity magnitude of a supersonic gas jet in its subsonic region (Ma<1) can be written as

$$\frac{u_{cl}}{u_0} = K_2 \frac{d_e}{L_G} \quad (1)$$

where u_{cl} is the centreline gas jet velocity (m·s^{-1}), u_0 is the released velocity at the nozzle exit (m·s^{-1}), d_e is the diameter at the nozzle exit (m), L_G is the distance between the liquid bath surface to the nozzle tip (m), and K_2 = 6.4 is a constant (Cheslak et al., 1969). The model predicted data were found in good agreement with the calculated velocity from Eq. (1) as shown in Fig. 2b.

3.2 Main blowing process

To simulate the main blowing process, an oxygen flow rate of 55,000 *Nm^3/hr* was used. Two lance head designs differing in number of nozzles and angle of inclination, were used to determine the effect of flow pattern on the potential wear prone zones. *Lance*1 comprised of 6 CD nozzles with an inclination of 17.30° relative to the lance centreline while *Lance*2 had 5 nozzles with an inclination angle of 15°. The Lance1 design produced Ma ~ 2.10, jet velocity, V ~ 502 m/s, and temperature T_s ~ -117 °C at the nozzle exit while *Lance2* design produced Ma ~ 1.97, jet velocity V ~ 482 m/s, and temperature T_s ~ -107 °C. The flow induced high shear stress is thought to contribute to the wearing of the lining.

3.2.1 Hydrodynamic behaviour inside the furnace

Fig. 3 presents the temporal evolution of the early stage of gas-liquid interface deformation during the jet impingement process in the *Lance*1 case, where a lance gap, gap between the nozzle exits and surface of molten bath, L_G = 2.0 m was maintained. At a very early stage (t ~ 0.05 s) a surface wave formed at the slag-gas interface due to the downward jet impingement. As time advances, impinging gas jets deforms the slag interface, and a cavity is formed. With the increasing depth of the cavity, multiple ligaments formed at the edge of the cavity (t~0.4s). Due to the shearing action of the impinging gas jet, these ligaments tore off and produced droplets leading to slag splashing on the furnace walls. Sabah and Brooks (2014) reported three distinct modes of cavity formation namely dimpling, splashing, and penetration. CFD simulations showed that cavity formation enters the penetration mode at t~1.25 s. Similar interface deformation behaviour was observed in the cold model experiment (Sabah and Brooks, 2014) where compressed air was blown into a pool of water.

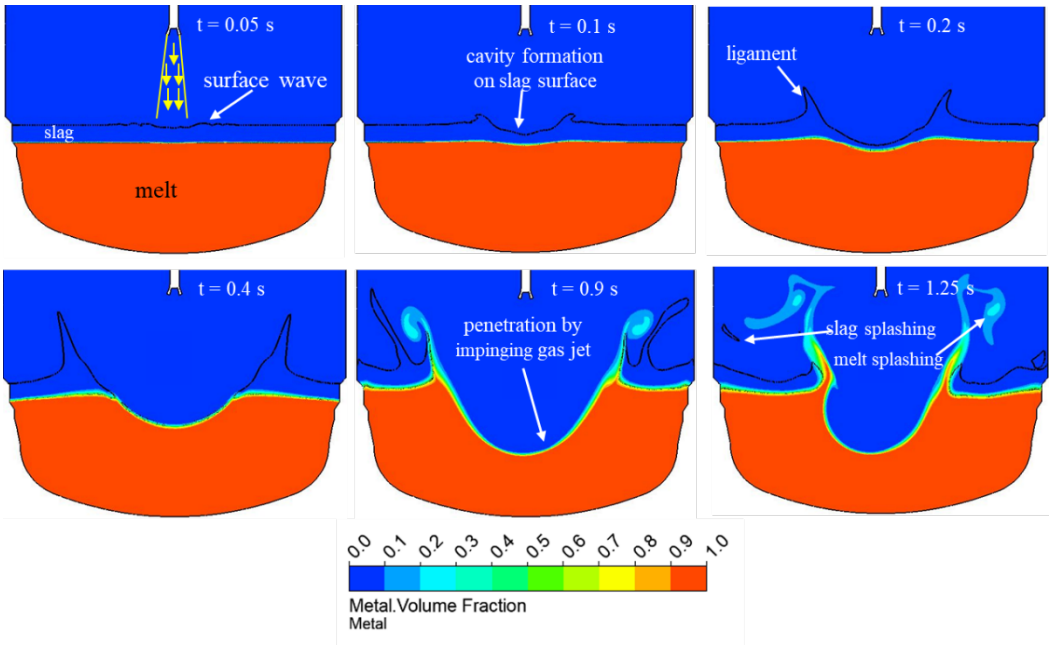

Fig 3: Interface deformation behaviour due to supersonic oxygen gas jet impingement in the main blowing process using *Lance1*.

As the oxygen blowing process continues, the slag-metal interface and molten bath movement become more dynamic. Due to the presence of a strong shear and relative velocity between the fluid layers, distinct surface waves are predicted due to Kelvin–Helmholtz instability which propagates across the entire bath surface. The oscillatory turbulent motions of the liquid phases along the furnace wall is expected to contribute to mechanical erosion of the refractory lining (Li et al., 2016b). The sloshing behaviour at the gas-slag, slag-melt or gas-melt interface also contribute to premature wear of refractory lining around the perimeter of the furnace.

3.2.2 Effect of lance designs on wall shear stress

The continuous undulatory motions of the gas-liquid interface induce shear stress on the furnace wall (Sun et al., 2022). This wall shear stress was computed as

$$\tau = \frac{\int (\mu+\mu_t)\frac{du}{dy}\,dA}{\int dA} \tag{2}$$

where u is the fluid velocity (m·s^{-1}) at the wall adjacent cell, and y is the height (m) of wall adjacent cell.

Fig. 4a presents the maximum shear stress on the refractory wall imparted by the slag and melt phase. The shear stress induced by slag phase at the right stadium and knuckle were computed as ~52 Pa and ~58 Pa, respectively. The wall shear stress induced at the right furnace wall by the melt phase was found more than three times higher compared to the slag phase. The computed shear stresses were as follow - right stadium ~ 168 Pa, right knuckle ~240 Pa, left stadium ~ 65 Pa, and left knuckle ~ 20 Pa.

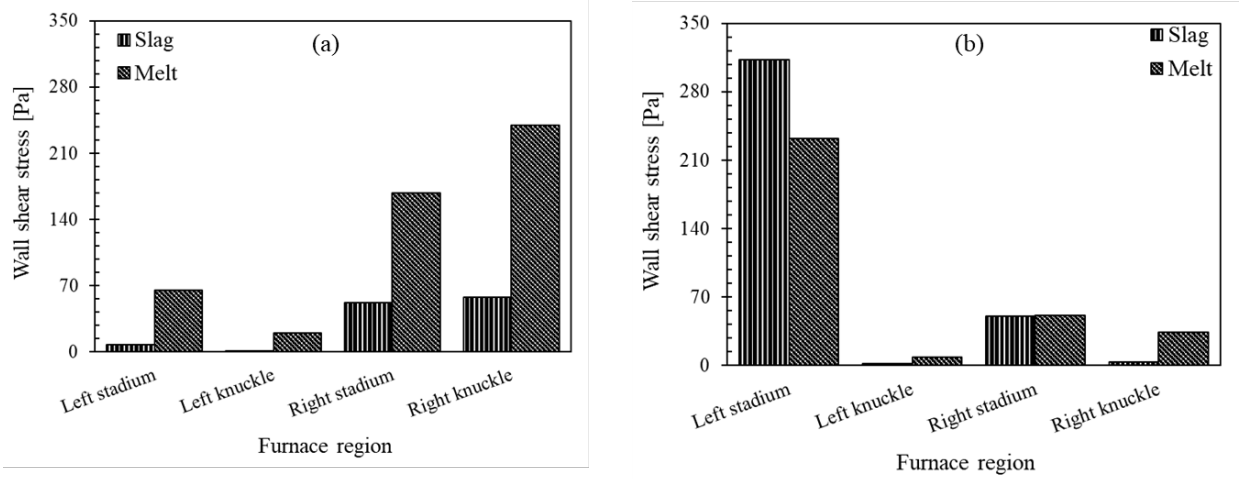

Fig 4: Shear stress induced by slag and melt on furnace wall in main blowing process using (a) *Lance1* and (b) *Lance2* designs.

The nozzle design and inclination angle were different for the lance *Lance2* compared to *Lance*1. Due to different jet momentum created by these two designs, both cavity profile and molten bath oscillatory behaviour were different in these two cases. For the case of *Lance2*, the lance gas was 2.15 m. The computed values of maximum shear stress on the refractory wall based on *Lance2* design case is shown in Fig. 4b. The continuous sloshing motions of the generated surface wave caused high wall shear stress at the left stadium region of the furnace. The maximum shear stress induced by slag were ~51 Pa at the right stadium and ~313 Pa at the left stadium. The computed maximum shear stress by melt phase were ~51 Pa at right stadium, ~34 Pa at right knuckle, and ~ 232 Pa at left stadium, respectively. These values were comparable with the suggested shear stress ~ 45 Pa in Fruehan (1998) required to form a crack on refractory surface. Model predicted potential wear prone zones agreed reasonably with the laser scan data obtained from the plant (not presented due to their confidentiality).

3.3 Slag splashing

Slag splashing cases were simulated by blowing nitrogen gas at a flow rate 11,600 *Nm^3/hr* and 250 *Nm^3/hr* through the top mounted lance and the bottom mounted tuyeres, respectively. Utilising these gas flow rates in the compressible flow model, *Lance*1 provided a sub-sonic velocity, *V* ~260 m/s, and temperature, T_s ~ -6 °C at the nozzle exit whereas *Lance2* provided a sub-sonic velocity *V* ~246 m/s, and T_s ~ -6 °C. The tuyeres produced a choked flow condition at sonic velocity *V* ~300 m/s at the tip and the corresponding temperature was T_s ~ -60 °C. Simulations were run accounting for three lance heights (L_H = 3.1, 2.8, and 2.1 m), two initial slag volume (2 and 4 m^3), and two lance designs (*Lance1* and *Lance2*). Gas was blown through two bottom tuyeres in all cases.

3.3.1 Hydrodynamic behaviour during slag splashing

Fig. 5 presents the transient hydrodynamic behaviour of downward gas jet interaction with the retained slag pool using *Lance*1 for three different lance positions and initial slag volume of 2 m^3. After being discharged from the nozzle exit, gas jets travel through a freeboard region and entrain the surrounding gas. The accumulation of turbulent entrainment leads to the radial expansion and the mixing of the jet boundaries (Li et al., 2015) which causes merging of two jets into a single jet and significant deviation from the respective nozzle axes (*t*~0.05 s). Waves are generated at the slag surface due to impingement of gas jets from the lance and cavity formation occurs within the slag pool due to bottom jetting from the tuyeres (*t*~0.05 s). The inside cavities expand with time and push the slag surface upwards along the walls (*t*~0.2 s). Finally, the slag pool ruptures into three parts (*t*~0.5 s). Gas jets move the separated slag mass towards the wall and form a thin coating layer on the wall (*t*~1 s). Due to the gravitational effect, the bulk slag moves back to the furnace floor (*t*~2 s).

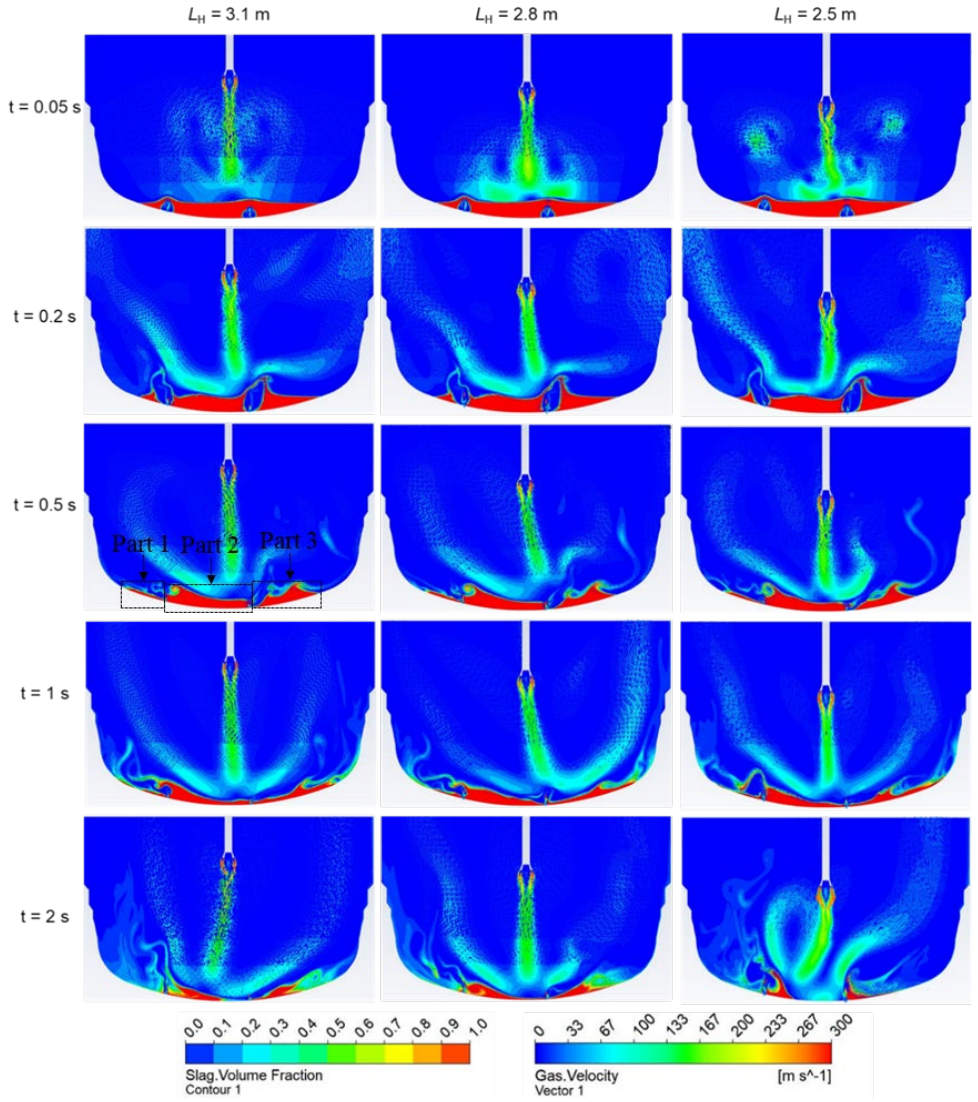

Fig 5: Unsteady interaction of gas jets with the retained slag (initial slag volume 2 m^3) for three lance positions using *Lance1*

Lowering the lance height from 3.1 m to 2.8 m, top gas jets impinge on the slag surface with a higher kinetic energy. Consequently, the gas jets push slag along the furnace wall much higher in both, left and right directions (t~1 s, L_H = 2.8 m) up to the stadium region. Further lowering the lance to 2.5 m, the higher energy jets completely rupture the slag pool and contacts the furnace floor (t~2 s).

3.3.2 Effect of lance position on slag coating

Fig. 6 presents the energy flux on the slag surface as a function of lance position for the two different lance designs. The energy flux on the slag surface was computed as:

$$\text{Energy flux} = \frac{\int \rho_g V^3 dA}{\int dA} \quad (3)$$

where ρ_g is the density (kg·m^{-3}) and V is the gas velocity (m·s^{-1}).

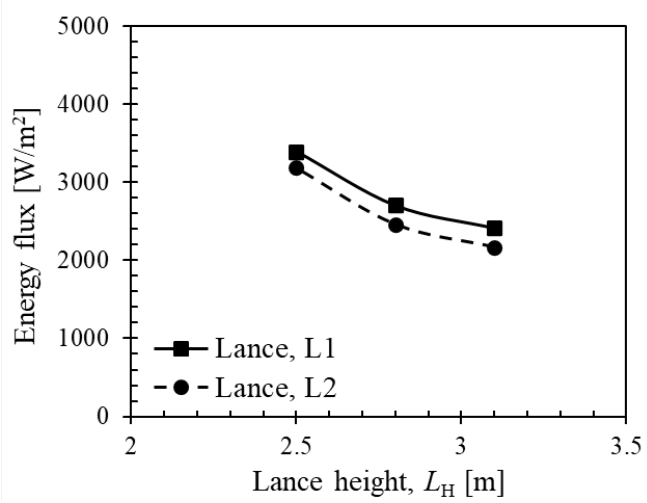

Fig 6: Energy flux on slag surface for different lance designs and lance positions

From Fig.6, it can be seen that the energy transfer rate per unit area on the slag surface decreased with the increase of lance height. The reason is that at lower lance height jet energy decay is lower due to low entrainment and the gas jet impinges on the slag surface at higher energy. At all lance heights, gas jets impinged on the slag pool with higher energy using *Lance*1 compared to *Lance*2 as shown in Fig. 6. This is due to the higher gas jet velocity (velocity~260 m/s) released from *Lance*1 compared to *Lance*2 (velocity~246 m/s).

3.3.3 Effect of initial slag mass on slag coating

Fig. 7 presents the coated area on refractory wall covered by slag splashing as a function of the lance height for different initial slag volume using *Lance*1. The coated area reported here is the average coated area of left and right walls of the furnace. Only knuckle, stadium, and barrel walls were considered to compute the coated area which is given as:

$$\text{Coated area (\%)} = \frac{\int \varphi dA_{wall}}{\int dA_{wall}} \times 100 \quad (3)$$

where φ is the slag phase and A_{wall} is the area of the wall.

In Fig.7a, for a fixed gas flow rate ~ 11,600 $Nm^3 \cdot hr^{-1}$ and slag volume 2 m^3, ~53% of knuckle area was coated at lance position of 3.1 m. No significant change in coating formation on the knuckle region was found for subsequently lowering the lance position to 2.8 m and then to 2.5 m. Intuitively, a higher coating area would be expected due to lance position closer to the free surface allowing the gas jets to impinge on the slag surface with higher kinetic energy. This however did not happen in the simulations because of insufficient slag mass present in the system which could not be fully utilised to coat the furnace wall. Moreover, lowering the lance position, the high energy gas jet ruptured the slag pool leading to contact with the furnace floor and energy dissipation.

Increasing slag volume from 2 m^3 to 4 m^3, at the highest lance position (L_H = 3.1 m), coated area at knuckle region increased by ~27.7%. Due to the increased slag volume, gas jets moved a higher amount of slag along the furnace wall and thus the coated area increased. At lance position of 2.8 m, the coated area at the knuckle region increased by ~43%. The coated area however decreased by ~20% for lowering lance position from 2.8 m to 2.5 m. This is again attributed to increasing energy flux on slag surface which led to complete penetration of the slag pool and contact with the furnace floor resulting in loss of jet energy and reduction in the amount of slag splashed (Mills et al., 2005).

Fig. 7b shows the coated area at the stadium region for the variation of lance height. At L_H = 3.1m, ~12% of stadium region coated at the initial slag volume 2 m^3. For lowering the lance height, the coated area at this region increased slightly which were obtained as follow: ~15% at L_H = 2.8 m and ~16% at L_H = 2.5 m. Although lowering lance height produces higher energy flux on slag pool, the amount of slag was not enough to travel to the stadium region. Increasing the slag volume 4 m^3, the coated area increased slightly which were as follow: ~14% at L_H = 3.1 m, ~17% at L_H = 2.8 m, and ~14% at L_H = 2.5 m.

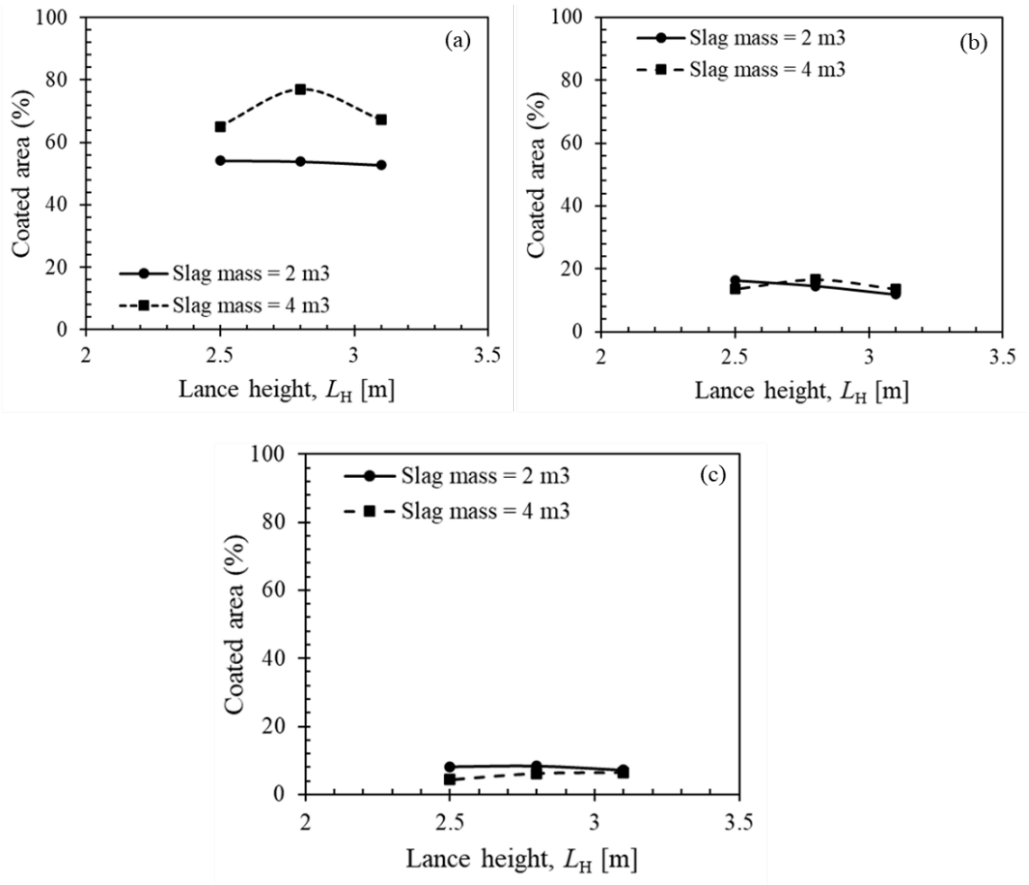

Fig 7: Variation of coated area on (a) knuckle wall, (b) stadium wall, and (c) barrel wall for the variation of lance height and initial slag volume utilizing *Lance1*.

Utilising the initial slag volume of 2 m^3, the coated area at barrel region remains almost the same (~8%) at all considered lance positions (Fig. 7c). Increasing slag volume to 4 m^3 caused the coated area to decrease slightly which was ~6% at lance position L_H = 3.1 m and L_H = 2.8 m. Further lowering it at L_H = 2.5 m, the coated area was only ~4%.

Fig. 8 presents the effect of *Lance2* on coated area for the variation of lance height and initial slag volume. Using slag volume of 2 m^3, coated area at knuckle region decreased slightly for lowering the lance height which were as follow: ~53% at L_H = 3.1 m, ~50% at L_H = 2.8 m, and ~44% at L_H = 2.5 m. The increase of slag volume aided to achieve a higher coated area for all lance heights. By lowering the lance position from L_H = 3.1 m to L_H = 2.8 m, coated area at the knuckle region increased

by ~22%. For further lowering lance position from L_H = 2.8 m to L_H = 2.5 m, coated area decreased by ~9%.

*Lance*2 provided a similar coating performance at the stadium region (Fig. 8b) and barrel region (Fig. 8c) as *Lance*1. For slag volume of 2 m^3, coated area in the stadium region decreased by lowering lance height (~16 % at L_H = 3.1 m, ~13% at L_H = 2.8 m, and ~10% at L_H = 2.5 m). Increasing initial slag volume to 4 m^3, the coated area remained almost the same at all lance positions (~12% at L_H = 3.1 m, ~12% at L_H = 2.8 m, and ~16% at L_H = 2.5 m). In the barrel region, the coated area was ~10% for all lance positions using initial slag volume of 2 m^3. However, increasing slag volume to 4 m^3, ~7% of the barrel area was coated for all lance positions.

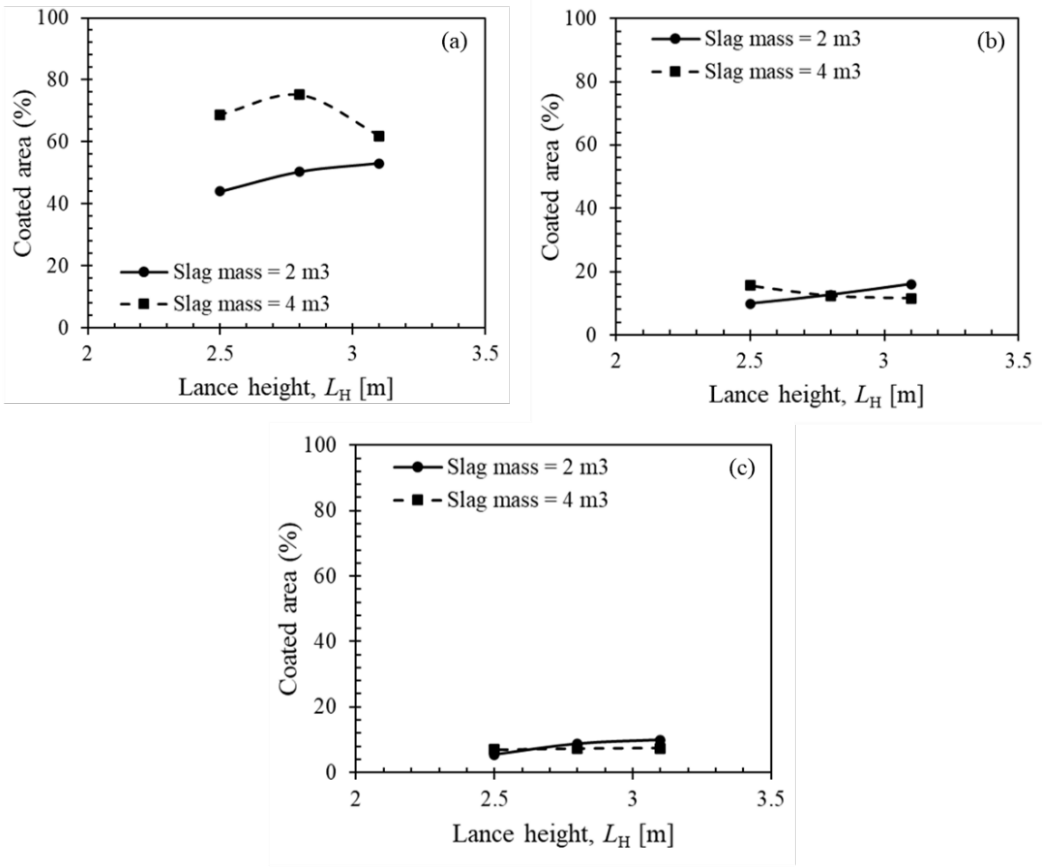

Fig 8: Variation of coated area on (a) knuckle wall, (b) stadium wall, and (c) barrel wall for the variation of lance height and initial slag volume utilizing *Lance2*.

3.3.4 Effect of tuyere location on slag coating

Fig. 9 shows the effect of tuyere location on coating formation on the refractory lining for the gas injection using *Lance1* and initial slag volume 4 m^3. Both tuyeres were located on either side of the furnace centreline, however *Tuyere2* is located closer to the furnace centreline (Fig. 9a) compared to *Tuyere1*. The slag pool was completely ruptured at the tuyere locations and formed three separate parts because of gas jet-slag surface interactions. Due to the location of *Tuyere2*, part 3 contained higher slag mass compared to part 1. Both top and bottom gas jets aided movement of the slag mass (part 3) toward the right wall and formed a coating. However, due to less slag mass present in part 1, coating formation at the left region is lower compared to the right part. This result reflects in Fig. 9b for all lance positions. At L_H = 2.8 m, ~64% of left knuckle area was coated whereas ~90% of right knuckle area was coated. A similar dependency of tuyere location on droplet generation was observed by (Qinglin, 1990).

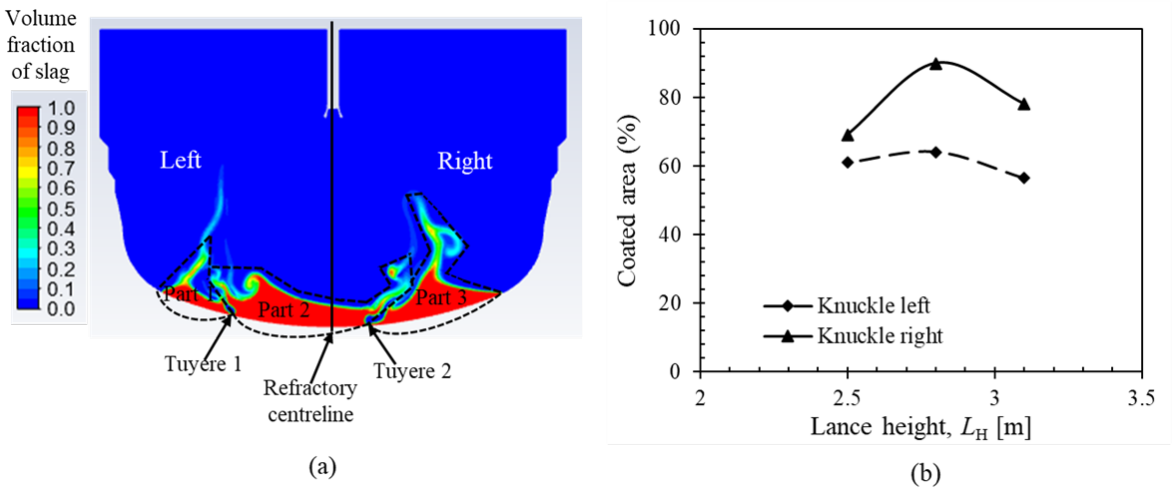

Fig 9: (a) Location of tuyere at the furnace bottom and (b) effect of tuyere location on coating formation using *Lance1* and initial slag volume 4 m^3.

CONCLUSIONS

In this study, CFD modelling was performed using actual plant data to identify the potential wear prone zones on the inner walls of an industrial scale BOS furnace during the main blowing process and determine the efficacy of slag splashing to coat these wear prone zones. The findings from these simulations are summarised as follow:

(1) The potential wear prone zones were characterised by the wall shear stress distribution for the two lance designs - *Lance1* and *Lance2* comprising 6 and 5 nozzles. The five-nozzle configuration produced larger stress compared to the six-nozzle configuration. Model predicted potential wear prone zones were left stadium, right stadium, and right knuckle, which agreed well with the plant data.

(2) Simulation of slag splashing produced almost the same coated area in the knuckle region for both lance head design at the higher lance position. The five-nozzle configuration however produced a slightly higher coated area at the stadium and barrel region compared to the six-nozzle one.

(3) Utilising a larger initial slag volume of 4 m^3, optimal lance position was found to be 2.8 m in both lance head design cases which produced maximum coated area at the knuckle and stadium region. However, *Lance1* design was found to contribute slightly higher coating performance compared to *Lance2*.

(4) The tuyere position had a strong influence on coating formation. The coating area on the right knuckle was found to be greater than the left knuckle area due to proximity of the *Tuyere2* to furnace axis compared to *Tuyere1*.

ACKNOWLEDGEMENTS

Funding from the Australian Research Council Industrial Transformation Research Hubs Scheme (Project Number IH130100017) is gratefully acknowledged.

REFERENCES

ALAM, M., NASER, J. & BROOKS, G. 2010. Computational Fluid Dynamics Simulation of Supersonic Oxygen Jet Behavior at Steelmaking Temperature. *Metallurgical and Materials Transactions B,* 41**,** 636-645.

BARRON, M., HILERIO, I. & MEDINA, D. 2015. *Slag Splashing in a Basic Oxygen Furnace under Different Blowing Conditions*.

CHESLAK, F. R., NICHOLLS, J. A. & SICHEL, M. 1969. Cavities formed on liquid surfaces by impinging gaseous jets. *Journal of Fluid Mechanics,* 36**,** 55-63.
DRAIN, P. B. 2018. *The effect of titanium on phosphorus removal during Basic Oxygen Steelmaking.* PhD, UNIVERSITY OF WOLLONGONG.
FRUEHAN, R. J. 1998. *The making, shaping, and treating of steel,* Pittsburgh, PA, AISE Steel Foundation.
LEÃO, P. M. G. C., RODRIGUES, E. F., DA SILVA, C. A., DA SILVA, I. A. & SESHADRI, V. 2016. Influence of Physical Properties of Slag and Operational Parameters on Slag Splashing Process in an Oxygen Convertor: Proceedings of the 10 th International Conference on Molten Slags, Fluxes and Salts.
LEE, M. S., O'ROURKE, S. & MOLLOY, N. A. 2001. Preferential refractory wear in top blown basic oxygen furnace. *Ironmaking & Steelmaking,* 28**,** 244-249.
LI, M., LI, Q., KUANG, S. & ZOU, Z. 2016a. Computational Investigation of the Splashing Phenomenon Induced by the Impingement of Multiple Supersonic Jets onto a Molten Slag–Metal Bath. *Industrial & Engineering Chemistry Research,* 55**,** 3630-3640.
LI, M., LI, Q., KUANG, S. B. & ZOU, Z. 2015. Coalescence Characteristics of Supersonic Jets From Multi-Nozzle Oxygen Lance in Steelmaking BOF. *steel research international,* 86**,** 1517-1529.
LI, Q., LI, M., KUANG, S. B. & ZOU, Z. 2016b. Understanding Characteristic of Abrasion of Refractory Lining Caused by Bath Oscillation in BOF Steelmaking. *JOM,* 68**,** 3126-3133.
LUOMALA, M. J., FABRITIUS, T. M. J., VIRTANEN, E. O., SIIVOLA, T. P., FABRITIUS, T. L. J., TENKKU, H., AUML & RKKI, J. J. 2002. Physical Model Study of Selective Slag Splashing in the BOF. *ISIJ International,* 42**,** 1219-1224.
MILLS, K. C., SU, Y., FOX, A. B., LI, Z., THACKRAY, R. P. & TSAI, H. T. 2005. A Review of Slag Splashing. *ISIJ International,* 45**,** 619-633.
MILLS, K. C., YUAN, L. & JONES, R. T. 2011. Estimating the physical properties of slags. *Journal of the Southern African Institute of Mining and Metallurgy,* 111**,** 649-658.
ODENTHAL, H. J., FALKENRECK, U. & SCHLÜTER, J. CFD simulation of multiphase melt flows in steelmaking converters. European Conference on Computational Fluid Dynamics, 2006 The Netherlands.
QINGLIN, H. 1990. *Fluid dynamics and droplet generation in the BOFsteelmaking proces.* Doctor of Philosophy University of Wollongong.
SABAH, S. & BROOKS, G. 2014. Splashing in Oxygen Steelmaking. *ISIJ International,* 54**,** 836-844.
SATTAR, M. A., NASER, J. & BROOKS, G. 2014. Numerical simulation of slag foaming on bath smelting slag (CaO–SiO2–Al2O3–FeO) with population balance modeling. *Chemical Engineering Science,* 107**,** 165-180.
SINELNIKOV, V., SZUCKI, M., MERDER, T., PIEPRZYCA, J. & KALISZ, D. 2021. Physical and Numerical Modeling of the Slag Splashing Process. *Materials,* 14**,** 2289.
SUN, J., ZHANG, J., LIN, W., FENG, X. & LIU, Q. 2022. Effect of Bottom Blowing Mode on Fluid Flow and Mixing Behavior in Converter. *Metals,* 12**,** 117.